



Minerva Access is the Institutional Repository of The University of Melbourne

Author/s:

ter Voert, CEM;Kour, RYN;van Teeffelen, BCJ;Ansari, N;Stok, KS

Title:

Contrast-enhanced micro-computed tomography of articular cartilage morphology with ioversol and iomeprol

Date:

2020-12

Citation:

ter Voert, C. E. M., Kour, R. Y. N., van Teeffelen, B. C. J., Ansari, N. & Stok, K. S. (2020). Contrast-enhanced micro-computed tomography of articular cartilage morphology with ioversol and iomeprol. *Journal of Anatomy*, 237 (6), <https://doi.org/10.1111/joa.13271>.

Persistent Link:

<https://hdl.handle.net/11343/276027>

1

2 DR. KATHRYN STOK (Orcid ID : 0000-0002-0522-4180)

3

4

5 Article type : Original Paper

6

7

8 **Contrast-enhanced micro-computed tomography of articular cartilage morphology with**
9 **ioversol and iomeprol**

10 Colet E.M. ter Voert, R.Y. Nigel Kour, Bente C.J. van Teeffelen, Niloufar Ansari, Kathryn S. Stok

11

12 Department of Biomedical Engineering, The University of Melbourne, Parkville, Australia

13

14 Corresponding author:

15 Kathryn S. Stok, PhD.

16 Department of Biomedical Engineering

17 The University of Melbourne

18 Parkville, Victoria 3010

19 Australia

20 Tel: +61 383449761

21 Email: kstok@unimelb.edu.au

22

23 **Running title:**

24 CECT imaging using ioversol and iomeprol

This is the author manuscript accepted for publication and has undergone full peer review but has not been through the copyediting, typesetting, pagination and proofreading process, which may lead to differences between this version and the [Version of Record](#). Please cite this article as [doi: 10.1111/JOA.13271](https://doi.org/10.1111/JOA.13271)

This article is protected by copyright. All rights reserved

1
2
3
4
5
6
7
8
9
10
11
12
13
14
15
16
17
18
19
20
21
22
23
24
25
26
27
28
29

Abstract

Non-ionic, low-osmolar contrast agents (CAs) used for computed tomography, such as Optiray (ioversol) and Iomeron (iomeprol), are associated with reduced risk of adverse reactions and toxicity in comparison to ionic CAs, such as Hexabrix. Hexabrix has previously been used for imaging articular cartilage but has been commercially discontinued. This study aims to evaluate the efficacy of Optiray and Iomeron as alternatives for visualisation of articular cartilage in small animal joints using contrast-enhanced micro-computed tomography (CECT). For this purpose, mouse femora were immersed in different concentrations (20% - 50%) of Optiray 350 or Iomeron 350 for periods of time starting at five minutes. The femoral condyles were scanned *ex vivo* using CECT, and regions of articular cartilage manually contoured to calculate mean attenuation at each time-point and concentration. For both contrast agents, a 30% contrast agent concentration produced a mean cartilage attenuation optimally distinct from both bone and background signal, whilst 5-minute immersion times were sufficient for equilibration of CA absorption.

Additionally, plugs of bovine articular cartilage were digested by Chondroitinase ABC to produce a spectrum of glycosaminoglycan (GAG) content. These samples were immersed in CA, and assessed for any correlation between mean attenuation and GAG content. No significant correlation was found between attenuation and cartilage GAG content for either CAs. In conclusion, Optiray and Iomeron enable high-resolution morphological assessment of articular cartilage in small animals using CECT, however, they are not indicative of GAG content.

Keywords:

Optiray, Iomeron, cartilage imaging, EPIC- μ CT, CECT

Introduction

June 13, 2020

1 Osteoarthritis (OA), a chronic degenerative joint disease, is the most common joint disorder. The
2 increasing prevalence of OA and a desire to start treatment as early as possible highlights the need
3 for non-invasive accurate detection of joint damage at early stages of disease. This would minimise
4 disability and pain and improve quality of life (Silvast et al., 2009).

5 To detect structural changes in articular cartilage, there is need for morphological assessment of
6 the extracellular matrix (ECM). Needle probing, histology and stereophotographic techniques are
7 readily available for this purpose, however, they provide limited information, and can be
8 destructive and time-consuming. (Xie et al., 2009) Therefore, non-destructive medical imaging
9 alternatives including micro-Magnetic Resonance Imaging (microMRI) and micro-computed
10 tomography (microCT), are often used to visualise cartilage. (Watrín et al., 2001, Roberts et al.,
11 2003, Watrín-Pinzano et al., 2005) Since MRI has a limited spatial resolution for mouse cartilage,
12 focus has been shifted to microCT, which accomplish higher spatial resolution in a shorter
13 acquisition time (Xie et al., 2009, Bansal et al., 2010, Lin et al., 2016, Willett et al., 2016, Lakin
14 et al., 2016, Stok et al., 2016, Das Neves Borges et al., 2014).

15 Micro-CT is an x-ray based imaging technique, providing quantitative 3D analysis of tissues and
16 is widely used for microstructural analysis of mineralised tissues, such as bone. Although microCT
17 is a standard modality for preclinical bone assessment, (Laib et al., 2000, Bouxsein et al., 2010)
18 its usage for articular cartilage is limited due to the low effective atomic number of the tissue,
19 which results in a low attenuation of x-rays, and difficulty in distinguishing cartilage from
20 surrounding soft tissues (Lusic and Grinstaff, 2013). Using a contrast agent (CA) that diffuses into
21 the cartilage, it can compensate for poor radiopacity of cartilage and enables its visualisation by
22 microCT. Visualisation and detection of OA-induced structural changes in articular cartilage of
23 small animals is beneficial for investigating treatment and prevention methods, which can
24 potentially be translated to the human disease.

25 Many CAs, such as iodine- or metal-based agents, possess elements of high atomic number –
26 capable of greater X-ray absorption (Lusic and Grinstaff, 2013). Iodine-based CAs are widely used
27 in different forms; they are High-Osmolar Contrast Media (HOCM) or Low-Osmolar Contrast
28 Media (LOCM), ionic or non-ionic, and monomeric or dimeric. HOCMs have higher risk of
29 inducing toxic effects and CA-induced nephropathy than LOCMs (Aspelin, 2006).

1 Hexabrix (Ioxaglate) is an example of an ionic iodine-based LOCMs, which was used for clinical
2 (angiography) imaging. Hexabrix was first introduced for preclinical CECT imaging in 2006,
3 (Palmer et al., 2006) and has not only enabled visualisation of the cartilage tissue by microCT, but
4 also quantification of morphological features such as cartilage thickness and volume (Xie et al.,
5 2012, Kerckhofs et al., 2013), (Kotwal et al., 2012). It was also used for assessment of articular
6 cartilage sulphated glycosaminoglycan (sGAG) content, one of the main components of cartilage
7 ECM (Xie et al., 2009).

8 Proteoglycans (PGs) are ECM components that compromise approximately 5-10 % of the wet
9 weight of articular cartilage, (Palmer et al., 2006) and their loss is an early indicator of OA.
10 (Buckwalter and Mankin, 1998) Since most ionic iodinated-based CAs (such as Hexabrix) are
11 negatively charged, the CAs and negatively charged side groups of the PGs in cartilage repel each
12 other, resulting in poorer absorption of the CA into cartilages with high GAG content. This shows
13 as a negative correlation between CECT attenuation and GAG content, suggesting the use of ionic
14 CAs as a predictor of GAG content in articular cartilage (Bansal et al., 2010, Xie et al., 2010).

15 Although Hexabrix was used by researchers for preclinical cartilage imaging, this was not the
16 primary market. It was recently discontinued by the manufacturer and replaced by other existing
17 agents for clinical angiography, such as Optiray (ioversol).(Food and Drug Administration)
18 Optiray (Ioversol; $C_{18}H_{24}I_3N_3O_9$; Figure 1a)(National Center for Biotechnology Information) and
19 Iomeron (Iomeprol; $C_{17}H_{22}I_3N_3O_8$; Figure 1b) (National Center for Biotechnology Information)
20 are two commercially available non-ionic iodinated LOCMs. Non-ionic CAs are estimated to yield
21 5 times fewer adverse reactions than ionic agents, such as Hexabrix, and this makes them a better
22 candidate for CECT (Aspelin, 2006), (McClennan, 1990, Christiansen, 2005).

23 In this study, we show the efficacy of Optiray and Iomeron for articular cartilage visualisation by
24 CECT. The primary aim of this study is to assess the viability of these two contrast agents for *ex*
25 *vivo* evaluation of cartilage morphology in mouse femoral articular cartilage using CECT. The
26 second aim of this study is to determine whether a correlation exists between GAG content and
27 CECT attenuation using Optiray or Iomeron.

28

29 **Materials & Methods**

30 **Specimen preparation**

June 13, 2020

1 For assessment of articular cartilage morphology with Optiray and Iomeron, femora were dissected
2 from excess 10-week old BALB/c mice carcasses from the Biomedical Sciences Animal Facility
3 at the University of Melbourne (n=12 per group). After removing the surrounding soft tissues, the
4 samples were stored in phosphate buffered saline (PBS) containing 1% protease inhibitor, at 4°C.
5 For assessment of CA attenuation, Ø5 mm plugs were cored from bovine femoral cartilage
6 acquired from an abattoir (n = 1, retired breeder). To create a spectrum of GAG content within the
7 cartilage samples, samples were treated with Chondroitinase ABC (Ch.ABC; Sigma-Aldrich, St.
8 Louis, MO, USA). Three groups (n = 10 per group) were studied for each CA: (i) control group
9 with no GAG digestion; (ii) 8 hours GAG digestion (8h-group); and (iii) 30 hours GAG digestion
10 (30h-group).

11

12 **Optiray and Iomeron for morphological assessment**

13 A schematic of the morphological assessment of cartilage using Optiray and Iomeron is shown in
14 Figure 2.

15 *Incubation protocol*

16 For assessment of cartilage morphology, Optiray 350 (Mallinckrodt, St. Louis, MO, USA) and
17 Iomeron 350 (Bracco Imaging, Colleretto Giacosa, TO, Italy) were used, both containing 350
18 mg/mL organically bound iodine. Different CA dilutions and immersion times were tested to
19 determine the optimal conditions for CECT imaging. For each CA, four concentrations of 70, 105,
20 140, and 175 mg Iodine/mL were tested by preparing 20, 30, 40, and 50% dilutions of CA in PBS,
21 respectively.

22 *MicroCT scanning and analysis*

23 Three samples (n=3) were scanned for each concentration of CA. For each sample, femoral
24 condyle was pre-scanned with microCT (immersion time = 0 minutes), then immersed in 2 mL of
25 CA solution at 37°C for cumulative times of 5, 10, 15, 30 and 60 minutes (total 6 scans for each
26 sample). Following each immersion, the femoral condyle was pat dry and scanned.

27 Samples were scanned in air using microCT (μ CT50, Scanco Medical, Bruttisellen, Switzerland).
28 Projections were acquired at a voxel size of 12 μ m, 55 kVp, 57 μ A, 0.5 mm Al filter, high

June 13, 2020

1 resolution, and 200 ms integration time. The femur was secured in the scanning tube to ensure the
2 longitudinal axis was positioned vertically. To prevent dehydration, the scanning tube contained a
3 small amount of PBS at the base, and the tube was sealed with parafilm.

4 For a set of scans of each femoral condyle, a cartilage mask volume was manually contoured and
5 then registered to the other 5 scans to ensure they all have a consistent volume of interest. This
6 approach was chosen over a threshold segmentation approach to ensure low attenuating data was
7 not excluded from the analysis, and the boundary between cartilage and bone was consistent
8 independent of CA concentration. Mean CECT attenuation and standard deviation of the mask
9 volume for each sample was calculated for each time point and concentration. Mean CECT
10 attenuation and standard deviation are calculated as the average greyscale value (out of total
11 32767) of all voxels in the mask volume using the *histogram* function in Scanco Medical's image
12 processing software (IPL v5.42).

13

14 **Assessment of the correlation between CECT Attenuation and GAG content**

15 A schematic of the preparation and analysis of correlation between CECT Attenuation and GAG
16 content is shown in Figure 3.

17 *GAG digestion*

18 Chondroitinase ABC (Ch.ABC), a GAG specific hydrolase, was used for enzymatic digestion of
19 bovine cartilage GAGs to small oligosaccharides to create a spectrum of GAG content. (Suzuki et
20 al., 1968, Otsuki et al., 2008) Each sample was immersed in 3 mL Ch.ABC digestion solution (0.1
21 U/mL in 50 mM Trisma-base, 60 mM NaOAc, 0.02% BSA, pH 8.0) at 37°C for a specified
22 digestion time (8 or 30 hours). After 8 hours, the samples (8h-group) were pat dry and stored at -
23 80°C. After 30 hours, samples from both 8h- and 30h-groups were washed with 10 mL containing
24 1% Antibiotic Antimycotic (A/A) (Sigma-Aldrich, St. Louis, MO, USA) in ultrapure water for 24
25 hours at 4°C, 750 RPM. After washing, samples were stored at 4°C in fresh 1% A/A solution.

26 *MicroCT scanning and analysis*

27 Following GAG digestion, smaller cores were punched from each sample to obtain Ø3 mm cores
28 with matching Ø5 mm outer rings. The inner core was immersed in CA as described below (where
29 $n = 5/\text{concentration}/\text{digestion time}$), whilst the outer ring was used to determine GAG content.

June 13, 2020

1 (Nimeskern et al., 2016) For CECT imaging, Iomeron 350 and Optiray 350 solutions were
2 prepared in concentration ratios of 30% and 20% in PBS, respectively, to ensure rapid
3 equilibration.

4 The inner core of each sample was immersed in the CA for 5 minutes at room temperature.
5 MicroCT scans were performed at a voxel size of 4 μm , 70 kVp, 57 μA , 0.5 mm Al filter, high
6 resolution, and 300 ms integration time.

7 After scanning, images for each sample were segmented by thresholding the cartilage from the
8 background using a grey-scale attenuation of 100 HU. Post-processing was conducted by creating
9 a solid mask of the cartilage volume after thresholding, from which mean and standard deviation
10 grey-scale attenuation in the sample was calculated.

11 *GAG content assay*

12 The wet weight of the outer ring of each sample was measured prior to lyophilisation for 24 hours.
13 All remaining GAG was extracted with 1 mg/mL papain enzyme (Sigma-Aldrich, P4762, St.
14 Louis, MO, USA) in papain buffer (20 mM sodium phosphate, 5 mM EDTA, 2 mM DTT, pH 6.8)
15 at 60°C for 8 hours. GAG content of each sample was assessed in two replicates, using 1,9-
16 dimethylmethylene blue (DMMB) (Sigma-Aldrich, 341088, St. Louis, MO, USA) colorimetric
17 assay. A microplate reader (Thermo Fisher Multiskan FC, Vantaa, Finland) was used to conduct
18 UV-Visible Spectroscopy, by measuring absorbance of each sample in triplicate at 520 nm.
19 Chondroitin-4-sulfate (Sigma-Aldrich, C4384, St. Louis, MO, USA) from shark cartilage was used
20 to produce a standard curve plotting GAG content against absorbance, with concentrations ranging
21 from 1 to 10 $\mu\text{g}/\text{mL}$ of GAG dissolved in papain buffer.

22 *Statistical analysis*

23 To determine optimal immersion time and concentration, CECT attenuation at 60-minutes
24 immersion was considered the equilibrium state, while significantly different CECT attenuation to
25 bone and no-contrast cartilage were considered required for good segmentation. A two-factor
26 analysis of variance was performed to test for significance between immersion timepoints and
27 concentrations, as well as any interaction between them. Post hoc comparisons were performed
28 using Bonferroni's test, or in the case of unequal variances, Tamhane's T2 test. Levene's test of
29 equality was used to determine the error variance. In this way, the earliest equilibrium time was

1 determined for each CA concentration, and the optimal concentration to delineate the cartilage
2 from other structures (i.e. bone and no-contrast cartilage P-values < 0.05 were considered
3 statistically significant.)

4 To investigate the correlation between GAG content and CECT attenuation, F-tests for equality of
5 variances were executed to evaluate if the variances differed between each group that was
6 measured in triplicate by UV-Visible spectroscopy. Following this, a t-test with equal or unequal
7 variances, dependent on the F-test outcome, was used to compare the two replicates from each
8 sample to identify significant differences. Significant difference was defined as $p < 0.01$. A 99%
9 confidence interval was chosen since assays groups were taken from the same sample and no
10 significant difference should be present. The relationship between CECT attenuation and GAG
11 content was evaluated by linear regression analysis, $p < 0.05$. Statistical analysis was performed
12 with SPSS Statistics (v24, IBM, NY, USA).

13

14 **Results**

15 *Optiray for morphological assessment*

16 The optimal immersion time for each concentration of CA was defined as the earliest scan-time
17 showing no significant difference in CECT attenuation compared to the 60-minute immersion
18 scan. Figure 4a shows the change in CECT attenuation over time using four concentrations of
19 Optiray 350. No significant difference in attenuation was found from 5 minutes through to 60
20 minutes for all Optiray 350 concentrations (mean \pm SD: 20%: 3423 \pm 772 vs 4227 \pm 850; 30%:
21 5266 \pm 943 vs 6375 \pm 127; 40%: 6101 \pm 1882 vs 7321 \pm 846; and 7659 \pm 564 vs 8434 \pm 353, for
22 5 vs 60 minutes, respectively). Therefore, samples immersed for these times were considered be
23 at equilibrium for the respective concentrations.

24 For morphological analysis of cartilage, the cartilage should have an attenuation different from the
25 bone after immersion in CA. To identify the best concentration of CA for morphological
26 assessment, CECT attenuation at the earliest equilibrium time for each concentration of CA was
27 compared to that of subchondral bone and no-contrast cartilage, using the average attenuation of
28 bone (22.4%, 7340 units) and no-contrast cartilage (7%, 2294 units) (Figure 4b). Attenuation of

1 contrast-enhanced cartilage was found to be significantly different ($p < 0.05$) to both no-contrast
2 cartilage and bone for 30% (5-min) concentration (mean \pm SD: 5266 ± 943).

3 *Iomeron for morphological assessment*

4 Figure 4c shows the change in cartilage attenuation over time using the four concentrations of
5 Iomeron 350. There was also no significant difference between 5 minutes through to 60 minutes
6 for all Iomeron concentrations (mean \pm SD: 20%: 3656 ± 2474 vs 4211 ± 2774 ; 30%: 4180 ± 966
7 vs 5991 ± 216 ; 40%: 6925 ± 811 vs 8831 ± 592 ; and 8530 ± 346 vs 9423 ± 44 , for 5 vs 60 minutes,
8 respectively).

9 Figure 4d shows the CECT attenuation at the earliest equilibrium time(s) for each concentration
10 compared to bone and no-contrast cartilage. Using Iomeron 350, attenuation of contrast-enhanced
11 cartilage was found to be significantly different ($p < 0.05$) to both no-contrast cartilage and bone
12 for the 30% at 5-min (mean \pm SD: 4180 ± 966) and 50% at 5-min (mean \pm SD: 8530 ± 346) cases
13 (Figure 4d).

14 Figure 5 shows representative microCT images of cartilage using 20% (5-min), 30% (5-min), 40%
15 (5-min) and 50% (5-min) Optiray (Figure 5a) and Iomeron 350 (Figure 5b). While Figure 6 shows
16 matching histograms for the yellow insets boxes in Figure 5. In this work, contouring cartilage
17 when using lower contrast agent concentrations (20%, 30%), was found to be easier compared to
18 higher concentrations (40%, 50%). This is supported by the histograms, which – while not bimodal
19 – show more low-attenuating signal (<7340 units) that corresponds to the contrast signal in the
20 cartilage.

21 *Correlation between CECT attenuation and GAG content*

22 To investigate the correlation between GAG content and CECT attenuation of bovine articular
23 cartilage, linear regression for CECT attenuation using Iomeron (Figure 7a) and Optiray (Figure
24 7b) versus GAG content were plotted. One sample from the Optiray control group was excluded
25 from the correlation assessment as the t-test showed a significant difference ($p = 0.002$) in GAG
26 content between the triplicate measurements of this sample.

27 CECT attenuation values for Optiray were in the range of 4200 to 6000 units, while values varied
28 with Iomeron from 4500 to 7000. The regression plot of Optiray measured an R^2 value of 0.0172
29 and p-value of 0.49, whilst Iomeron gave an R^2 value of 0.0065 and p-value of 0.67. This indicates

June 13, 2020

1 that for both CAs, no significant correlation was found between CECT attenuation and GAG
2 content.

3

4 **Discussion**

5 This study shows that Optiray and Iomeron, two non-ionic LOCMs, increase attenuation of
6 articular cartilage in microCT scans, whilst enabling distinction between cartilage and bone. Both
7 CA concentration and immersion time were shown to affect the quality of cartilage visualisation.
8 Our results showed no correlation between CECT attenuation and GAG content of cartilage using
9 Iomeron and Optiray.

10 MicroCT imaging can produce high resolution, non-destructive 3D evaluation of articular cartilage
11 morphology. Hexabrix is an ionic LOCM contrast, used for preclinical CECT imaging and
12 arthrography (Xie et al., 2009). Despite its effectiveness in CECT, Hexabrix was withdrawn from
13 the market by the manufacturer in 2015 (Food and Drug Administration). Alternative non-ionic
14 LOCMs, including Optiray and Iomeron, have the same indications as Hexabrix, making them
15 prime candidates for its replacement in CECT imaging.

16 To seek a replacement for Hexabrix, we performed CECT using two clinically available non-ionic
17 CAs, Iomeron and Optiray, to evaluate morphology of mouse femoral articular cartilage *ex vivo*.

18 In preparing scan protocols, it is necessary to define equilibrium time to ensure a consistent uptake
19 of the contrast solution by the cartilage tissue. (Xie et al., 2012, Kotwal et al., 2012) For both
20 Optiray 350 and Iomeron 350, equilibration was achieved from 5 minutes for all concentrations
21 (20-50%) in mouse femoral cartilage. This is similar to equilibration times reported for other CAs
22 used for CECT imaging of cartilage: 6.7 minutes for Hexabrix (Kotwal et al., 2012) and 6.2
23 minutes for CA4+ in fresh mouse cartilage. (Lakin et al., 2016) These results also highlight that
24 although high concentrations of CA results in higher attenuation of cartilage in scanned images,
25 more time before imaging is not needed to reach equilibrium.

26 To assess joint morphology, the contrast of the cartilage should be distinctly different to that of
27 adjacent bone tissue. Ideally, this provides a bimodal histogram, allowing for a global threshold to
28 be applied to extract the various tissues for easy segmentation of different tissues. (Kotwal et al.,
29 2012) For the earliest immersion time of each concentration, mean CECT attenuation of contoured
30 cartilage was compared to bone and no-contrast cartilage. Our results showed that cartilage
31 immersed in higher concentrations (40% and 50%) of Optiray 350 and Iomeron 350 had a similar

1 attenuation to bone (22.4%, 7340 units), suggesting that higher concentrations of these CAs are
2 not suitable for morphological assessment of cartilage. However, 20 and 30% of Optiray 350 and
3 30% of Iomeron 350 (105 mg Iodine/mL) produced distinctly different contrast to bone, enabling
4 a reliable segmentation and quantification of cartilage and bone in CECT images. The iodine
5 content of this concentration (105 mg/mL) is similar to iodine content of the optimal concentration
6 of Hexabrix, 128 (mg I/mL). (Xie et al., 2009) .

7 Separating the peaks of the histogram is achieved by using different concentrations of the CA
8 solution. However, since there are other soft tissues present in addition to the cartilage which also
9 absorb the contrast agents this makes threshold-based tissue segmentation challenging (Figure 6).
10 In this case, additional manual contouring is often also required to segment cartilage and exclude
11 other soft tissues from assessment (Willett et al., 2016, Kotwal et al., 2012, Lakin et al., 2016). In
12 this work, we found samples immersed in lower concentrations, such as 30% of Iomeron 350 and
13 20 and 30% of Optiray 350, were easier to segment than higher concentrations (40%, 50%). Based
14 on these data, the optimal concentration and immersion time for morphological assessment of joint
15 using the two CAs is 30% (105 mg Iodine/mL) and 5 minutes for Iomeron 350 and 30% (105 mg
16 Iodine/mL) and 5 minutes for Optiray 350.

17 Hexabrix (ioxaglate) is an anionic CA that distributes inversely proportional to the negatively
18 charged GAGs in ECM. Although ionic CAs can be used for measuring GAG loss in tissues, due
19 to the electrostatic repulsion with GAGs, there is a low magnitude of attenuation in images. On
20 the other hand, cationic CAs bind proportionally to the negatively charged GAGs. However, their
21 strong electrostatic binding increases the time it takes for the body to clear the CA, and results in
22 increased risk of possible adverse reactions. In microCT, attenuation intensities of ionic CAs, such
23 as Hexabrix, (Xie et al., 2010) correlate with cartilage GAG content and that can be used as an
24 indication of the development of OA at early stages. The second aim of this work was to determine
25 whether a correlation exists between CECT attenuation of Optiray and Iomeron and cartilage GAG
26 content. Since Optiray and Iomeron are uncharged, it was hypothesized that no qualitative
27 relationship would be present between CECT attenuation and the GAG content. The concentration
28 and immersion time for both CAs were chosen based on the morphological assessment study, with
29 adjustments in immersion time to offset the absence of subchondral bone, and solution
30 concentration to target an attenuation value of approximately 4000 HU – slightly lower than the
31 midpoint of no-contrast cartilage and bone CT attenuation in Figure 4. Our results supported our

1 hypothesis, showing that unlike Hexabrix and CA4+ (Bansal et al., 2010) (Xie et al., 2010, Palmer
2 et al., 2006, Nickmanesh et al., 2018, Yoo et al., 2011, Cockman et al., 2006, Kallioniemi et al.,
3 2007), there is no correlations between Optiray and Iomeron CECT attenuation and GAG content
4 of cartilage (Figure 7). This indicates that although Optiray and Iomeron are promising agents for
5 morphological assessment of cartilage, they cannot be used as indicators of GAG-loss related to
6 OA.

7 Achieving diversity of GAG content was limited by the inherent characteristics of cartilage located
8 at different parts of the bovine femoral head. Although randomly selected, in the Optiray
9 correlation study it was observed that nine of the ten samples of the 30-hour GAG digested group
10 were totally GAG depleted. In contrast, in the Iomeron study only three of the ten samples were
11 totally GAG depleted. Chondroitinase ABC does not display a linear enzymatic activity, so
12 optimising digestion protocols to achieve more diversity in GAG content would be challenging.
13 However, even so, it is unlikely to change the finding that there is no significant correlation
14 between GAG content and CECT attenuation.

15 It can be observed in Figures 4 and 7, that Iomeron appears to have more variability in CECT
16 attenuation than Optiray. Further investigation of this phenomenon was outside the scope of this
17 study. However, most contrast agents of this kind are defined by their surface charge (and size).
18 Since both Optiray and Iomeron are non-ionic and do not have electrostatic interactions with
19 cartilage components, they may have other chemical interactions where they bind tighter or are
20 trapped within the tissue in Optiray and not Iomeron. This requires further investigation.

21 *Conclusion*

22 In this work, optimal concentration and immersion times for Optiray and Iomeron were identified
23 to provide high resolution morphology of femoral articular cartilage of the mouse by microCT.
24 Although these CAs show comparable result to the discontinued Hexabrix, no relationship was
25 observed between CECT attenuation and GAG content. This suggests that although Optiray and
26 Iomeron can provide valuable morphological data of cartilage, other CAs are needed to replace
27 discontinued agent, Hexabrix, for detecting GAG loss with OA at early stages using CECT.

28

29 **Acknowledgements**

June 13, 2020

1 This research was partially supported by the Australian Government through the Australian
2 Research Council's Discovery Projects funding scheme (project DP180101838). BVT and CTV
3 were each supported by a student stipend from the Technical University of Eindhoven, The
4 Netherlands. Thanks to Dr Julia Gregory for preparing figures 2 and 3. None of the authors have
5 any conflict of interest.

6

7 **Author Contributions Statement:**

8 All authors designed the experiments, analysed and interpreted the data. BVT, CTV and NRYK
9 performed the experiments. CTV, NRYK, NA and KSS wrote the manuscript, and BVT critically
10 reviewed the manuscript. KSS designed the study and provided resources for all experiments. All
11 authors have read and approved the final submitted manuscript.

12

13 **Data Availability Statement:**

14 The data that support the findings of this study are available from the corresponding author upon
15 reasonable request.

16 **References**

17 ASPELIN, P. 2006. Why choice of contrast medium matters. *European Radiology Supplements*, 16, D22-
18 D27.

19 BANSAL, P. N., JOSHI, N. S., ENTEZARI, V., GRINSTAFF, M. W. & SNYDER, B. D. 2010. Contrast enhanced
20 computed tomography can predict the glycosaminoglycan content and biomechanical properties
21 of articular cartilage. *Osteoarthritis Cartilage*, 18, 184-91.

22 BOUXSEIN, M. L., BOYD, S. K., CHRISTIANSEN, B. A., GULDBERG, R. E., JEPSEN, K. J. & MULLER, R. 2010.
23 Guidelines for assessment of bone microstructure in rodents using micro-computed tomography.
24 *Journal of bone and mineral research : the official journal of the American Society for Bone and*
25 *Mineral Research*, 25, 1468-86.

26 BUCKWALTER, J. A. & MANKIN, H. J. 1998. Articular cartilage: degeneration and osteoarthritis, repair,
27 regeneration, and transplantation. *Instr Course Lect*, 47, 487-504.

28 CHRISTIANSEN, C. 2005. X-ray contrast media--an overview. *Toxicology*, 209, 185-7.

29 COCKMAN, M. D., BLANTON, C. A., CHMIELEWSKI, P. A., DONG, L., DUFRESNE, T. E., HOOKFIN, E. B., KARB,
30 M. J., LIU, S. & WEHMEYER, K. R. 2006. Quantitative imaging of proteoglycan in cartilage using a
31 gadolinium probe and microCT. *Osteoarthr Cart*, 14, 210-4.

June 13, 2020

- 1 DAS NEVES BORGES, P., FORTE, A. E., VINCENT, T. L., DINI, D. & MARENZANA, M. 2014. Rapid, automated
2 imaging of mouse articular cartilage by microCT for early detection of osteoarthritis and finite
3 element modelling of joint mechanics. *Osteoarthr Cartilage*, 22, 1419-28.
- 4 FOOD AND DRUG ADMINISTRATION. *Guerbet Group; Withdrawal of Approval of Two New Drug*
5 *Applications* [Online]. Available: [https://www.federalregister.gov/documents/2017/04/24/2017-](https://www.federalregister.gov/documents/2017/04/24/2017-08179/guerbet-group-withdrawal-of-approval-of-two-new-drug-applications)
6 [08179/guerbet-group-withdrawal-of-approval-of-two-new-drug-applications](https://www.federalregister.gov/documents/2017/04/24/2017-08179/guerbet-group-withdrawal-of-approval-of-two-new-drug-applications) [Accessed Jan 7,
7 2019].
- 8 KALLIONIEMI, A. S., JURVELIN, J. S., NIEMINEN, M. T., LAMMI, M. J. & TOYRAS, J. 2007. Contrast agent
9 enhanced pQCT of articular cartilage. *Phys Med Biol*, 52, 1209-19.
- 10 KERCKHOFS, G., SAINZ, J., WEVERS, M., VAN DE PUTTE, T. & SCHROOTEN, J. 2013. Contrast-enhanced
11 nanofocus computed tomography images the cartilage subtissue architecture in three
12 dimensions. *Eur Cell Mater*, 25, 179-89.
- 13 KOTWAL, N., LI, J., SANDY, J., PLAAS, A. & SUMNER, D. R. 2012. Initial application of EPIC-muCT to assess
14 mouse articular cartilage morphology and composition: effects of aging and treadmill running.
15 *Osteoarthritis Cartilage*, 20, 887-95.
- 16 LAIB, A., BAROU, O., VICO, L., LAFAGE-PROUST, M. H., ALEXANDRE, C. & RUGSEGGER, P. 2000. 3D micro-
17 computed tomography of trabecular and cortical bone architecture with application to a rat
18 model of immobilisation osteoporosis. *Med Biol Eng Comput*, 38, 326-32.
- 19 LAKIN, B. A., PATEL, H., HOLLAND, C., FREDMAN, J. D., SHELOFSKY, J. S., SNYDER, B. D., STOK, K. S. &
20 GRINSTAFF, M. W. 2016. Contrast-enhanced CT using a cationic contrast agent enables non-
21 destructive assessment of the biochemical and biomechanical properties of mouse tibial plateau
22 cartilage. *Journal of Orthopaedic Research*, 34, 1130-1138.
- 23 LIN, K. H., WU, Q., LEIB, D. J. & TANG, S. Y. 2016. A novel technique for the contrast-enhanced microCT
24 imaging of murine intervertebral discs. *Journal of the mechanical behavior of biomedical*
25 *materials*, 63, 66-74.
- 26 LUSIC, H. & GRINSTAFF, M. W. 2013. X-ray-computed tomography contrast agents. *Chem Rev*, 113, 1641-
27 66.
- 28 MCCLENNAN, B. L. 1990. Preston M. Hickey memorial lecture. Ionic and nonionic iodinated contrast
29 media: evolution and strategies for use. *American Journal of Roentgenology*, 155, 225-233.
- 30 NATIONAL CENTER FOR BIOTECHNOLOGY INFORMATION. 2019a. *PubChem Compound Database*.
31 *CID=3731* [Online]. Available: <https://pubchem.ncbi.nlm.nih.gov/compound/3731> [Accessed Jan.
32 7, 2019].

June 13, 2020

- 1 NATIONAL CENTER FOR BIOTECHNOLOGY INFORMATION. 2019b. *PubChem Substance Database*.
2 *SID=3741* [Online]. Available: <https://pubchem.ncbi.nlm.nih.gov/substance/3741> [Accessed Jan.
3 7, 2019].
- 4 NICKMANESH, R., STEWART, R. C., SNYDER, B. D., GRINSTAFF, M. W., MASRI, B. A. & WILSON, D. R. 2018.
5 Contrast-enhanced computed tomography (CECT) attenuation is associated with stiffness of
6 intact knee cartilage. *J Orthop Res*, 36, 2641-2647.
- 7 NIMESKERN, L., UTOMO, L., LEHTOVIITA, I., FESSEL, G., SNEDEKER, J. G., VAN OSCH, G. J., MULLER, R. &
8 STOK, K. S. 2016. Tissue composition regulates distinct viscoelastic responses in auricular and
9 articular cartilage. *J Biomech*, 49, 344-52.
- 10 OTSUKI, S., BRINSON, D. C., CREIGHTON, L., KINOSHITA, M., SAH, R. L., D'LIMA, D. & LOTZ, M. 2008. The
11 effect of glycosaminoglycan loss on chondrocyte viability: a study on porcine cartilage explants.
12 *Arthritis Rheum*, 58, 1076-85.
- 13 PALMER, A. W., GULDBERG, R. E. & LEVENSTON, M. E. 2006. Analysis of cartilage matrix fixed charge
14 density and three-dimensional morphology via contrast-enhanced microcomputed tomography.
15 *Proc Natl Acad Sci U S A*, 103, 19255-60.
- 16 ROBERTS, M. J., ADAMS, S. B., JR., PATEL, N. A., STAMPER, D. L., WESTMORE, M. S., MARTIN, S. D.,
17 FUJIMOTO, J. G. & BREZINSKI, M. E. 2003. A new approach for assessing early osteoarthritis in the
18 rat. *Anal Bioanal Chem*, 377, 1003-6.
- 19 SILVAST, T. S., JURVELIN, J. S., AULA, A. S., LAMMI, M. J. & TOYRAS, J. 2009. Contrast agent-enhanced
20 computed tomography of articular cartilage: association with tissue composition and properties.
21 *Acta Radiol*, 50, 78-85.
- 22 STOK, K. S., BESLER, B. A., STEINER, T. H., ESCUDERO, A. V. V., ZULLIGER, M. A., WILKE, M., ATAL, K.,
23 QUINTIN, A., KOLLER, B., MULLER, R. & NESIC, D. 2016. Three-Dimensional Quantitative
24 Morphometric Analysis (QMA) for In Situ Joint and Tissue Assessment of Osteoarthritis in a
25 Preclinical Rabbit Disease Model. *Plos One*, 11.
- 26 SUZUKI, S., SAITO, H., YAMAGATA, T., ANNO, K., SENO, N., KAWAI, Y. & FURUHASHI, T. 1968. Formation
27 of three types of disulfated disaccharides from chondroitin sulfates by chondroitinase digestion.
28 *J Biol Chem*, 243, 1543-50.
- 29 WATRIN-PINZANO, A., RUAUD, J. P., OLIVIER, P., GROSSIN, L., GONORD, P., BLUM, A., NETTER, P., GUILLOT,
30 G., GILLET, P. & LOEUILLE, D. 2005. Effect of proteoglycan depletion on T2 mapping in rat patellar
31 cartilage. *Radiology*, 234, 162-70.

- 1 WATRIN, A., RUAUD, J. P., OLIVIER, P. T., GUINGAMP, N. C., GONORD, P. D., NETTER, P. A., BLUM, A. G.,
2 GUILLOT, G. M., GILLET, P. M. & LOEUILLE, D. H. 2001. T2 mapping of rat patellar cartilage.
3 *Radiology*, 219, 395-402.
- 4 WILLETT, N. J., THOTE, T., HART, M., MORAN, S., GULDBERG, R. E. & KAMATH, R. V. 2016. Quantitative
5 pre-clinical screening of therapeutics for joint diseases using contrast enhanced micro-computed
6 tomography. *Osteoarthritis and Cartilage*, 24, 1604-1612.
- 7 XIE, L., LIN, A. S., GULDBERG, R. E. & LEVENSTON, M. E. 2010. Nondestructive assessment of sGAG content
8 and distribution in normal and degraded rat articular cartilage via EPIC-microCT. *Osteoarthr*
9 *Cartilage*, 18, 65-72.
- 10 XIE, L., LIN, A. S., KUNDU, K., LEVENSTON, M. E., MURTHY, N. & GULDBERG, R. E. 2012. Quantitative
11 imaging of cartilage and bone morphology, reactive oxygen species, and vascularization in a
12 rodent model of osteoarthritis. *Arthritis Rheum*, 64, 1899-908.
- 13 XIE, L., LIN, A. S., LEVENSTON, M. E. & GULDBERG, R. E. 2009. Quantitative assessment of articular cartilage
14 morphology via EPIC-microCT. *Osteoarthritis Cartilage*, 17, 313-20.
- 15 YOO, H. J., HONG, S. H., CHOI, J. Y., LEE, I. J., KIM, S. J., CHOI, J. A. & KANG, H. S. 2011. Contrast-enhanced
16 CT of articular cartilage: experimental study for quantification of glycosaminoglycan content in
17 articular cartilage. *Radiology*, 261, 805-12.

18

19 **Figure Legends**

20 Figure 1. Chemical structure of the contrast agent compounds (a) Optiray and (b) Iomeron.
21 (National Center for Biotechnology Information, National Center for Biotechnology Information)

22

23 Figure 2. An overview of the sample preparation, scan timeline, and data processing and analysis
24 tasks for assessing cartilage morphology using Optiray and Iomeron.

25

26 Figure 3. An overview of the sample preparation, DMMB assay, and microCT scanning and
27 analysis tasks for assessing GAG correlation with CECT attenuation for Optiray and Iomeron.

28

29 Figure 4. Mean CECT attenuation against time for each concentration of (a) Optiray 350 and (c)
30 Iomeron 350. Mean CECT attenuation for the earliest equilibrium time(s) for each (b) Optiray and
31 (d) Iomeron concentration, compared to bone (solid) and no-contrast cartilage (dashed). * and †

1 indicate significant difference to bone and no-contrast cartilage attenuation values, respectively (p
2 < 0.05).

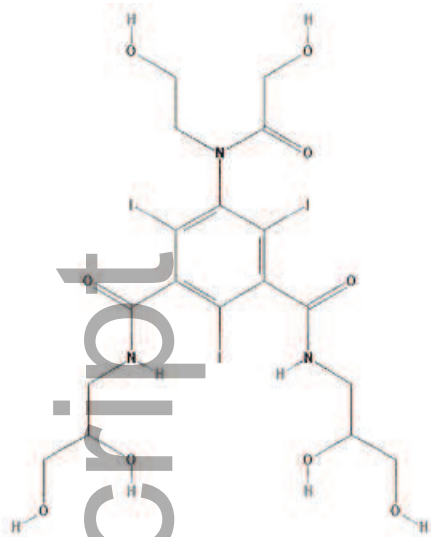
3

4 Figure 5. Representative CECT images of mouse cartilage using 20%, 30%, 40% and 50% of (a)
5 Optiray 350, and (b) Iomeron 350. Dashed region of interest insets are used to create histograms
6 in Figure 6.

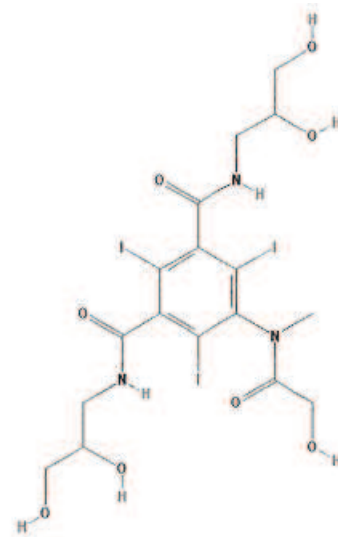
7

8 Figure 6. Histograms of mouse cartilage using 20%, 30%, 40% and 50% of (a) Optiray 350, and
9 (b) Iomeron 350 from dashed region of interest insets in Figure 5.

10 Figure 7. Linear regression plots of CECT attenuation using (a) Optiray and (b) Iomeron vs. GAG
11 content of bovine articular cartilage. The light blue shaded curve shows the 95% confidence
12 intervals for individual points and the dark blue shaded curve shows the 95% confidence interval
13 curve for the mean.



Optiray (loversol)



lomeron (lomeprol)

joa_13271_f1.tif

Author Manuscript

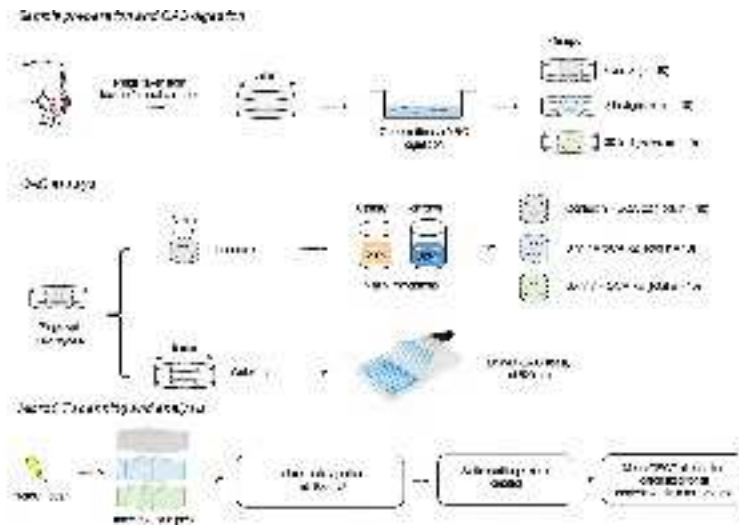
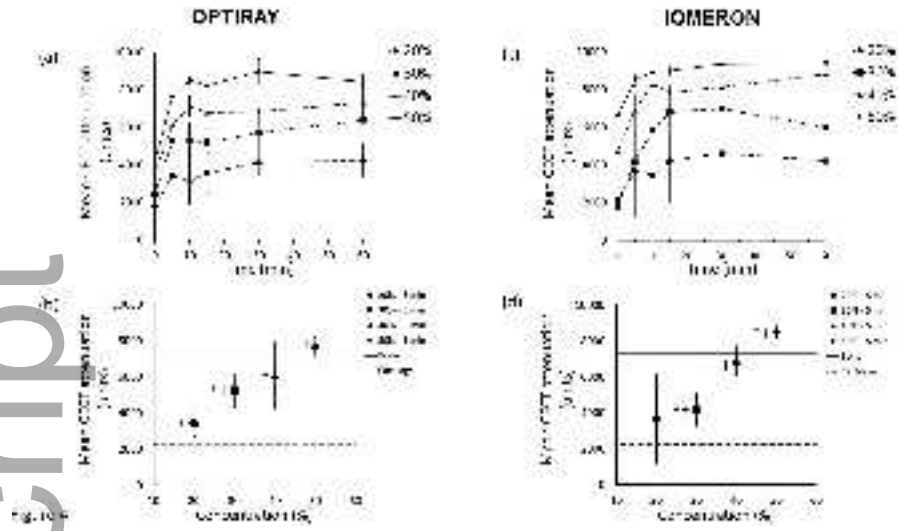
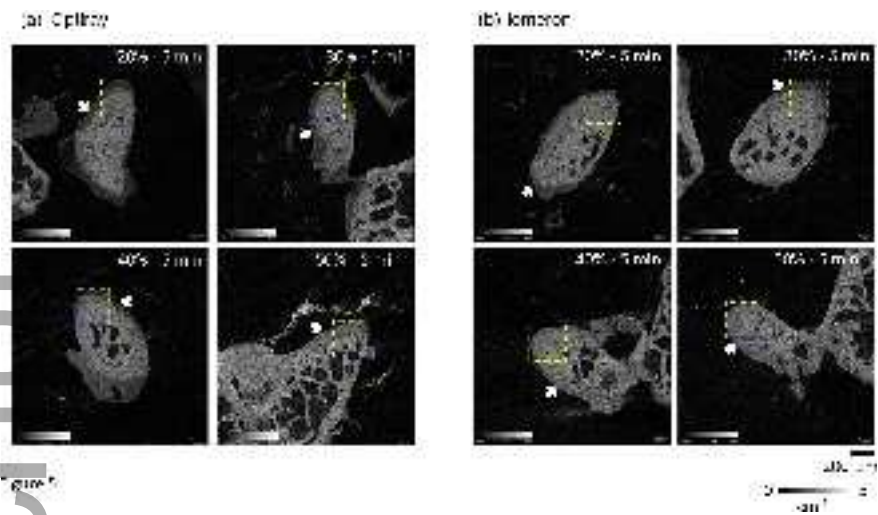


Fig. 10.3

joa_13271_f3.tif

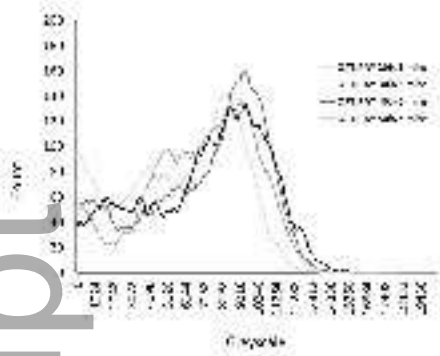


joa_13271_f4.tif

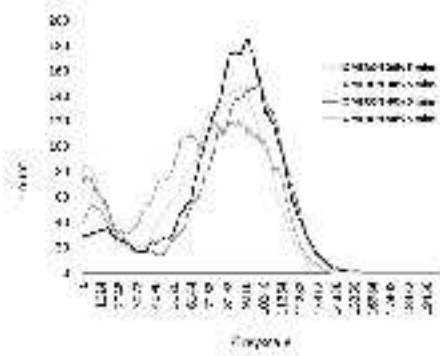


joa_13271_f5.tif

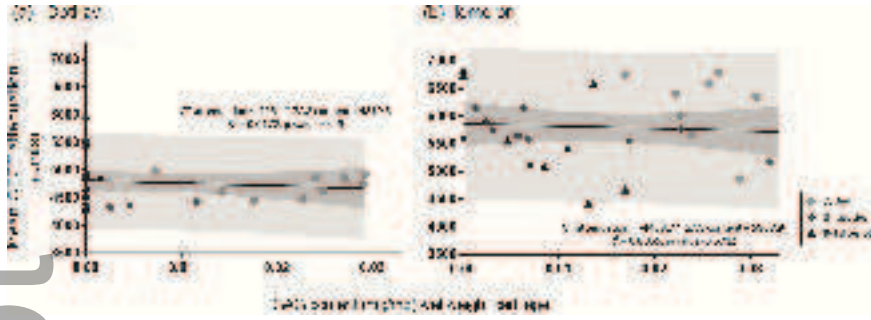
(a) Dpfray



(b) emeron



joa_13271_f6.tif



joa_13271_f7.tif